Received: 15 June 2020 | Revised: 22 September 2020 | Accepted: 24 September 2020

DOI: 10.1002/app.50087

ARTICLE

Applied Polymer SCIENCE WILEY

Effectiveness of the preparation of maleic anhydride grafted poly (lactic acid) by reactive processing for poly (lactic acid)/carbon nanotubes nanocomposites

Gleice Ellen Almeida Verginio[1] | **Thais Larissa do Amaral Montanheiro**[2] | **Larissa Stieven Montagna**[1] | **Juliano Marini**[3] | **Fabio Roberto Passador**[1]

[1]Federal University of São Paulo (UNIFESP), Polymer and Biopolymer Technology Laboratory (TecPBio), 330 Talim St., São José dos Campos, SP, Brazil

[2]Laboratory of Plasmas and Processes, Technological Institute of Aeronautics, Praça Marechal Eduardo Gomes, 50 - Vila das Acacias, São José dos Campos, SP, Brazil

[3]Federal University of São Carlos (UFSCar), Department of Materials Engineering, Rodovia Washington Luís, Km 235, São Carlos, SP, Brazil

Correspondence
Fabio Roberto Passador, Federal University of São Paulo (UNIFESP), Polymer and Biopolymer Technology Laboratory (TecPBio), 330 Talim St., São José dos Campos, SP 12231-280, Brazil.
Email: fabio.passador@unifesp.br

Abstract

An effective strategy to increase the properties of poly (lactic acid) (PLA) is the addition of carbon nanotubes (CNT). In this work, aiming to improve the surface adhesion of PLA and CNT a new compatibilizer agent was prepared by reactive processing, PLA grafted maleic anhydride (PLA-*g*-MA) using benzoyl peroxide and maleic anhydride. The effectiveness of the PLA-*g*-MA as a compatibilizer agent was verified for PLA/PLA-*g*-MA/CNT nanocomposites. PLA and PLA-*g*-MA samples were characterized by Fourier transform infrared spectroscopy (FT-IR) to confirm the grafting reaction of maleic anhydride on PLA chains and by rheological analysis to prove the changes in the matrix PLA after the graphitization reaction. Thermal (differential scanning calorimetry and thermogravimetric analysis), mechanical tests (Izod impact strength and tensile test), and morphological characterization were used to verify the effect of the compatibilizer agent. The preparation of PLA-*g*-MA by reactive extrusion processing proved satisfactory and the nanocomposites presented good thermal and mechanical properties. The addition of the PLA-*g*-MA also contributed to the greater distribution of CNT and can be used as an alternative for the production of PLA/CNT nanocomposites.

KEYWORDS

biopolymers and renewable polymers, thermoplastics, nanotubes, graphene, and fullerenes, functionalization of polymers

1 | INTRODUCTION

The mechanical performance of nanocomposites is usually affected by the weak interfacial adhesion between the polymer matrix and the nanofiller.[1] Several studies[2–6] show that the weak interface facilitates failure in the interfacial region due to inefficient strain transfer.

An interesting strategy to improve the interfacial adhesion in nanocomposites is the use of small quantities of compatibilizer agent to minimize the incompatibility between the polymer matrix and the nanofiller.[7] The compatibilizer agent is responsible for performing the interaction of immiscible components through functional groups.[6] The main functional groups used are maleic anhydride (MA)[8] and acrylic acid (AA).[9]

Maleic anhydride (MA) grafting thermoplastic polymers is typically used as a compatibilizer agent.[5,8,10–12] The MA group presents highly reactive with a wide variety of polymer chains and biological macromolecules.[5] Passador et al.[11] studied the influence of the addition of MA grafted

high-density polyethylene (HDPE-*g*-MA) and MA grafted linear low-density polyethylene (LLDPE-*g*-MA) in HDPE/LLDPE/nanoclay nanocomposites. The authors used a mixture of 50/50 wt% of these compatibilizer agents and observed improvements in the dispersion and distribution of the nanoclay in the polymer matrix. Moreover, it was also observed a stronger interaction and adhesion between the nanoclay and the polymer matrix. The authors used commercially compatibilizer agents.

However, for some systems, there is a lack of commercial compatibilizer agents, and it is necessary to develop new compatibilizer agents. One way for this development is through reactive processing. Braga et al.[8,10,13] prepared a MA grafted poly(trimethylene terephthalate) (PPT-*g*-MA) by a reactive extrusion process using benzoyl peroxide and MA. The effectiveness of the PTT-*g*-MA was verified for PTT/ABS (acrylonitrile butadiene styrene) blends and PTT/carbon nanotubes composites. The authors showed that the addition of PTT-*g*-MA is a good option to improve the thermal and mechanical properties of blends and nanocomposites based on PTT.

Greater challenges occur when preparing nanocomposites from a biodegradable polymer matrix. The use of biodegradable polymers is an effective alternative for the reduction of waste generated by plastic since biodegradable polymers generate short-lived residues compared to synthetic polymers.[14,15] However, there are no commercial compatibilizer agents available for these systems. Montanheiro et al.[5] produced MA grafted poly(hydroxybutyrate-*co*-hydroxyvalerate) (PHBV-*g*-MA) by reactive processing using dicumyl peroxide and MA. The compatibilizer agent presented low molecular weight without loss of thermal properties and can be used for PHBV nanocomposites.

In this way, the current work suggests the development of a new way to produce the compatibilizer agent based on poly (lactic acid) (PLA) by reactive processing. PLA is a biodegradable polymer, thermoplastic, obtained from natural origin, produced by renewable sources, and widely used in the packaging sector.[16,17] Despite its excellent properties, PLA has high fragility, rigidity, and low surface adhesion with the filler.[18,19] An effective strategy to increase the properties of PLA is the addition of carbon nanotubes (CNT). The CNT is composed of allotropic nanostructures of carbon and has excellent mechanical, electrical, and thermal properties.[20–23] However, to have good interfacial adhesion between PLA and CNT is necessary the addition of compatibilizer agent. One way to improve the interface of the nanocomposite is the introduction of functional groups into the main chain of PLA by reaction with vinyl monomers, such as MA and producing MA grafted PLA (PLA-*g*-MA). From the reaction between PLA and MA, reactive sites are generated and occur the formation of branches in the PLA main chain; the MA has dual reactivity, double bond free radical, and cyclic anhydride.[24,25]

The preparation of PLA-*g*-MA was investigated using different types of initiators and processing. Carlson et al.[25] prepared PLA-*g*-MA by reactive extrusion using MA and 2,5-dimethyl-2,5-di-(tertbutyperoxy) hexane as the free radical initiator. The samples were obtained varying two reaction temperatures, 180 and 200°C, with the initiator concentration between 0.0 and 0.5 wt%. During the extrusion process, a little degradation of the PLA backbone was observed. The effectiveness of the compatibilizer agent was verified for PLA/talc composites and high adhesion between the filler and PLA matrix was confirmed.

Can and Kaynak[26] prepared PLA-*g*-MA by twin-screw reactive extrusion using MA and dicumyl peroxide as the free radical initiator and the effectiveness was verified for PLA/titanium dioxide (TiO_2) composites. The addition of PLA-*g*-MA increases the tensile strength, the flexural modulus and the toughness of the composites. Nam and Son[27] prepared PLA-*g*-MA in a co-rotating twin screw extruder using MA and perkadox 14 as the radical initiator. In this case, the effectiveness was verified for PLA/polyamide 11 (PA 11) blends. The authors observed that the addition of PLA-*g*-MA decreased the interfacial energy and improved the interfacial adhesion between the two polymers.

Rigolin et al.[28] prepared PLA-*g*-MA using 1 phr of dicumyl peroxide as initiator and 2 phr of MA by reactive processing. The PLA-*g*-MA was successfully obtained, and the effectiveness was verified for PLA/coir fibers composites. The authors showed that the addition of PLA-*g*-MA as compatibilizer agent improved the interfacial adhesion between the coir fibers and PLA and increase the mechanical properties. Rigolin et al.[29] also investigated the effect of different peroxides on the physical and chemical properties of PLA-*g*-MA. The authors compared the effect of dicumyl peroxide and 2,5-dimethyl-2,5-di(t-butylperoxy) hexane (DHBP) as initiators. In addition, the authors verified several ratios between the initiator and MA. The compatibilizer agents were prepared by reactive processing. The use of DHBP as an initiator was slightly more efficient than the dicumyl peroxide in increasing the acidity of the PLA and these compatibilizer agents can be used for PLA-based systems.

Other strategies were used to improve the interfacial adhesion of PLA/CNT nanocomposites.[30] For example, the use of carboxylic-functionalized CNTs,[31] oxidized CNT (CNTs-COOH)[32] and functionalized CNTs with hydroxyl groups to polymerize L-lactide (CNT-*g*-PLLA) in PLA matrix.[33]

Grafting reactions is also performed in the PLA matrix or CNT, such as, grafting maleic anhydride in CNT (MA-*g*-CNT),[34] grafting PLLA onto the CNTs (PLLA-*g*-CNTs),[35] CNTs grafted with PLA chains (CNT-

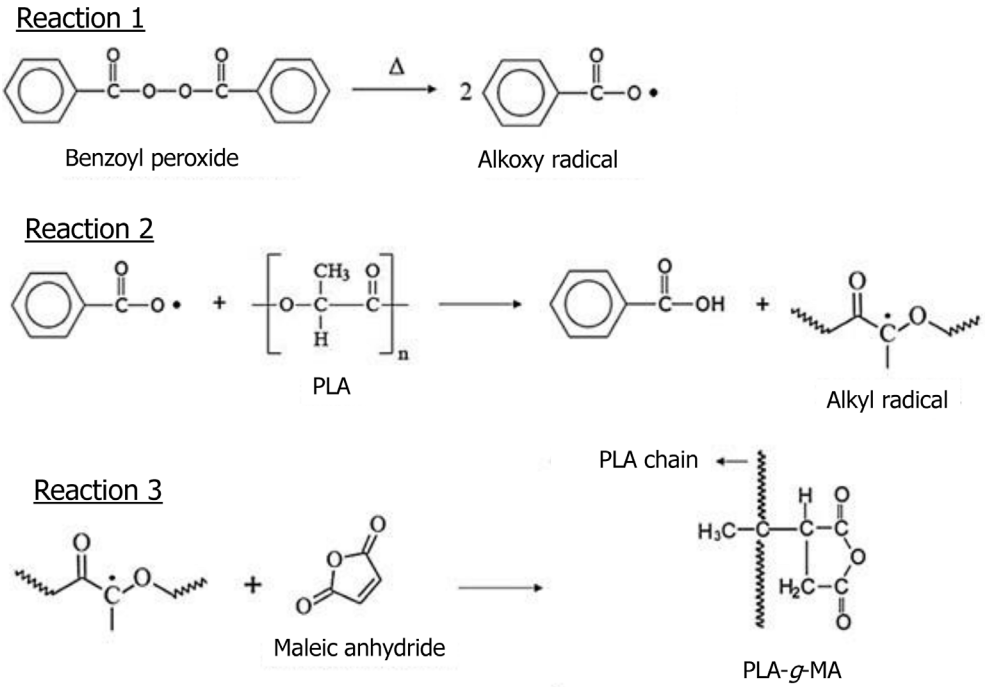

FIGURE 1 Grafting reactions to produce PLA-*g*-MA using benzoyl peroxide (BPO) as initiator and maleic anhydride (MA) as a monomer

g-PLAs) with the addition of carboxylic acid-functionalized CNT (CNT-COOH) to obtain PLA/CNT-*g*-PLA nanocomposites,[36] and hydroxyl-functionalized CNTs (CNT-OH) by a melt blending method[37] and modification CNT with maleic anhydride, methyl methacrylate and vinyltrimethoxysilane modifiers.[38]

In this work, PLA-*g*-MA was produced in a single step by reactive extrusion processing using benzoyl peroxide (BPO) as the initiator. The use of BPO as an initiator for the preparation of PLA-*g*-MA has not been reported. In addition, BPO has a lower cost compared to dicumyl peroxide which is usually used in the graphitization process. The effectiveness of the new compatibilizer agent prepared by reactive processing was verified for PLA/PLA-*g*-MA/CNT nanocomposites. Another goal was the analysis of the effect of different contents of PLA-*g*-MA in the thermal and mechanical properties, and morphological characterization of the nanocomposites.

2 | EXPERIMENTAL

2.1 | Materials

Poly (lactic acid) (PLA) was supplied by Nature Plast (France), with specification PLI 005 and density of 1.25 g/cm^3.

Maleic anhydride (MA) was used as a monomer and supplied by Sigma-Aldrich (USA) with 99% purity and the benzoyl peroxide (BPO) was used as initiator

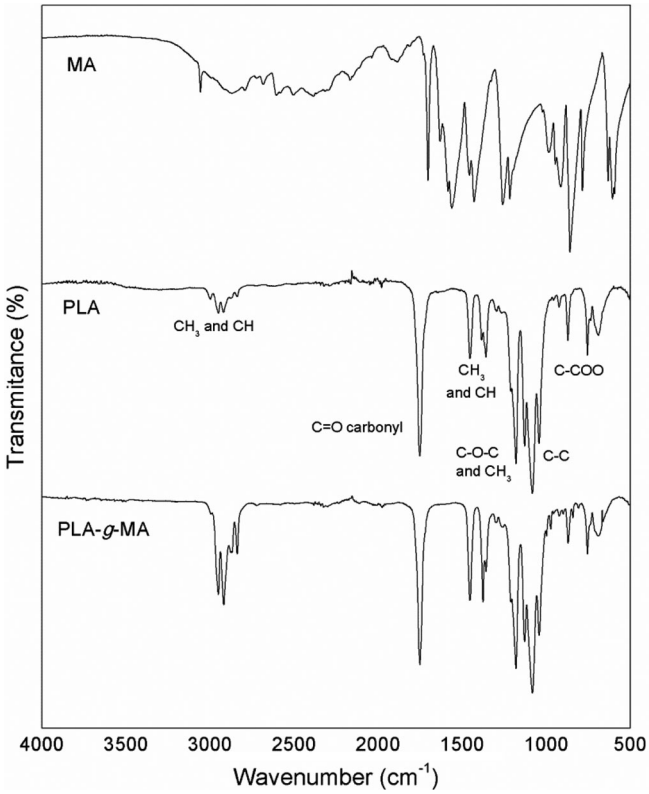

FIGURE 2 FT-IR spectra of maleic anhydride, PLA-*g*-MA and PLA (left) and zoom at region between 1050–780 cm^{-1} (right)

and supplied by Dinâmica Química Contemporânea (Brazil). Both reagents were used as received. Multiwall carbon nanotubes (CNT) were supplied by Nanocyl S. A. (Belgium) with 90% purity, average

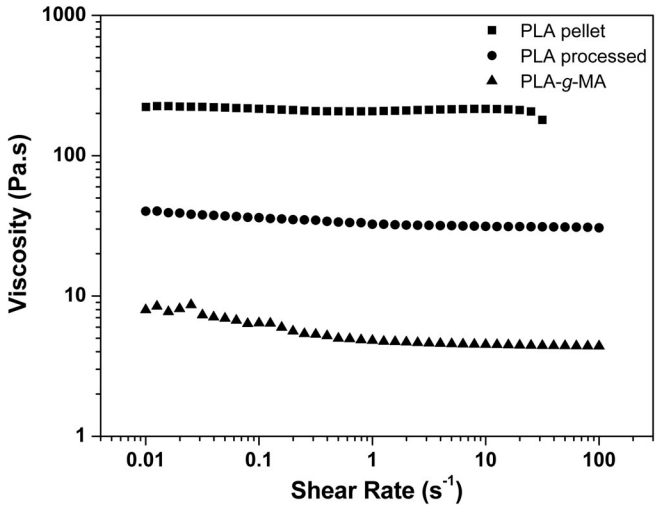

FIGURE 3 Viscosity curve as a function of the shear rate obtained by deformational rheometry of PLA, PLA pellet, and PLA-*g*-MA

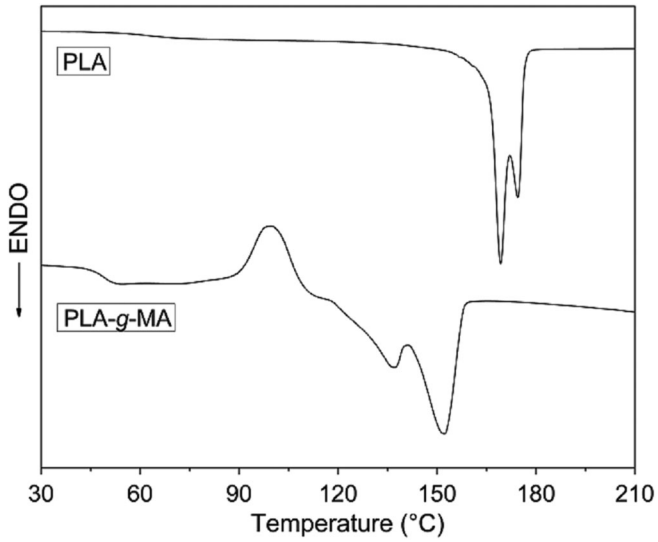

FIGURE 4 DSC curves of second heating of PLA and PLA-*g*-MA

diameter of 9.5 nm and length of 1.5 μm and high aspect ratio (L/D ~ 158).

2.2 | Reactive processing of PLA-*g*-MA

PLA was dried at 60°C in a vacuum oven (Shel LAB, model SVAC1E) for 12 h before the reactive processing. The reactive extrusion processes to prepare PLA-*g*-MA by melt-grafting were carried out in a co-rotational twin-screw extruder AX Plásticos, model AX16:40DR (L/D = 40, D = 16 mm), with screw rotation speed of 80 rpm and feeding in 25 rpm. The PLA-*g*-MA was prepared with 96.0 wt% of PLA, 2.0 wt% of BPO and 2.0 wt% MA. The temperature profile set was 165, 170, 170, 170 and 165°C from the first zone to the die. After the extrusion, the PLA-*g*-MA was pelletized and dried on a vacuum oven at 60°C for 12 h.

The same extrusion process was performed with neat PLA. The PLA after the extrusion process was named as PLA and the polymer before the extrusion process was named as PLA pellet.

2.3 | Characterization of PLA-*g*-MA

2.3.1 | FT-IR spectroscopy

PLA-*g*-MA, PLA and MA were analyzed Fourier transform infrared spectroscopy (FT-IR) using universal attenuated total reflection (UATR) accessory in a PerkinElmer Frontier equipment. The spectrum was acquired in transmittance mode by the accumulation of 24 scans with a range of 4000–500 cm^{-1}.

2.3.2 | Rheological characterization

The rheological behavior of PLA-*g*-MA, PLA, and PLA pellets was evaluated in a rotational controlled stress rheometer from TA Instruments, model ARG2. The steady-state viscosity was evaluated as a function of the shear rate in an inert nitrogen atmosphere at a temperature of 180°C, using parallel-plate geometry with 25 mm of diameter and gap of 1 mm. The delay before the measurement was determined from stress overshoot experiments performed at 180°C and 0.01 s^{-1} until constant stress was attained.

2.3.3 | Thermal characterization

The thermal properties of PLA and PLA-*g*-MA were analyzed by differential scanning calorimetry (DSC) and thermogravimetric analysis (TGA).

DSC tests were performed in a TA Instruments equipment, model Q2000 under nitrogen as the carrier gas in a constant flow of 50 mL/min. Approximately 10 mg of the sample was sealed in an aluminum DSC pan. The following experimental programming was used: (a) First heating cycle at 10°C min^{-1} from 0°C to 220°C; (b) Isotherm from 220°C, 3 min, to eliminate the heat history of the samples; (c) cooling at 10°Cmin^{-1} from 220°C to 0°C; (d) Second heating cycle at 10°C min^{-1}

reheated from 0°C to 220°C. The degree of crystallinity (X_c) was calculated according to Equation 1:

$$Xc\,(\%) = \frac{\Delta Hm - \Delta Hcc}{\Delta Hm^{\circ}}.100 \quad (1)$$

ΔH_m is the total melting enthalpy, ΔH_{CC} is the cold crystallization enthalpy and ΔH_m° is the theoretical heat fusion of 100% crystalline PLA, which was taken as 93 J/g.[39]

TGA was performed in Netzsch equipment, model TG 209 F1 Iris®. The samples (~10 mg) were carried out under a nitrogen atmosphere from room temperature to 800°C with a heating rate of 20°Cmin^{-1}.

TABLE 1 Thermal properties obtained by DSC analysis of the PLA and PLA-*g*-MA

	Second heating		
Samples	**T_g (°C)**	**T_{m1}(°C)**	**T_{m2} (°C)**
PLA	62	169	175
PLA-*g*-MA	49	137	152

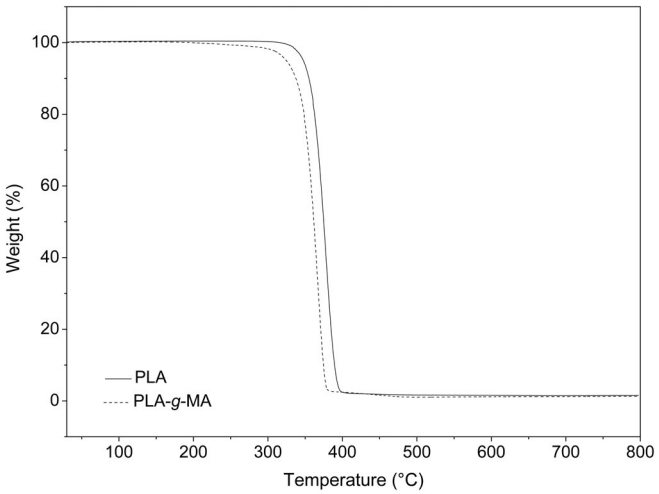

FIGURE 5 Thermal degradation behavior curves of PLA and PLA-*g*-MA

2.4 | Effectiveness of the compatibilizer agent in PLA/CNT nanocomposites

The effectiveness of the PLA-*g*-MA as a compatibilizer agent was verified for PLA/CNT nanocomposites. First, PLA and PLA-*g*-MA were dried at 60°C in a vacuum oven for 12 h before the extrusion process. PLA/PLA-*g*-MA/CNT nanocomposites with different contents of PLA-*g*-MA (0, 1 and 3 wt%) and 1 wt% of CNT[40,41] were processed using an AX Plásticos, model AX16:40DR co-rotational twin-screw extruder using a temperature profile of 165, 170, 170, 170 and165°C from the first section to the die, with a screw rotation speed of 120 rpm and feeding of 30 rpm. The nanocomposites were pelletized and dried at 60°C in a vacuum oven for 12 h.

After the extrusion process, thin films (0.23 mm) were prepared by hot press using a hydropneumatic press (MH Equipamentos Ltda, model PR8H) at 190°C with a pressure of 1 bar for 2 min. The thin films were used to tensile tests according to ASTM D 882–12.[42]

Standardized specimens for Izod impact strength tests according to ASTM D256-06[43] were pressed into 3.2 mm thick plates in a hydropneumatic press (MH Equipamentos Ltda, model PR8H) at 210°C with a pressure of 5 bars for 3 min.

2.5 | Characterization of PLA/PLA-*g*-MA/CNT nanocomposites

2.5.1 | Thermal characterization: DSC and TGA

DSC and TGA analyses of the nanocomposites were performed under the same equipment and conditions mentioned above.

2.5.2 | Mechanical characterization: Izod impact strength tests and tensile tests

Izod impact strength tests were carried out according to ASTM D256-06[43] and were performed on a CEAST/Instron Izod impact testing machine (model 9050), with 1 to 2.75 J hammer. It was used 1 J hammer for PLA neat

TABLE 2 The initial thermal degradation temperature (T_{onset}), the thermal degradation temperature of 10, 50, and 90% of weight loss, the maximum weight loss rate temperature ($T_{máx}$) and the end thermal degradation temperature (T_{endset})

Sample	T_{onset} (°C)	$T_{10\%}$ (°C)	$T_{50\%}$ (°C)	$T_{90\%}$ (°C)	$T_{máx}$ (°C)	T_{endset} (°C)
PLA	355	355	375	390	379	390
PLA-*g*-MA	343	337	362	375	367	378

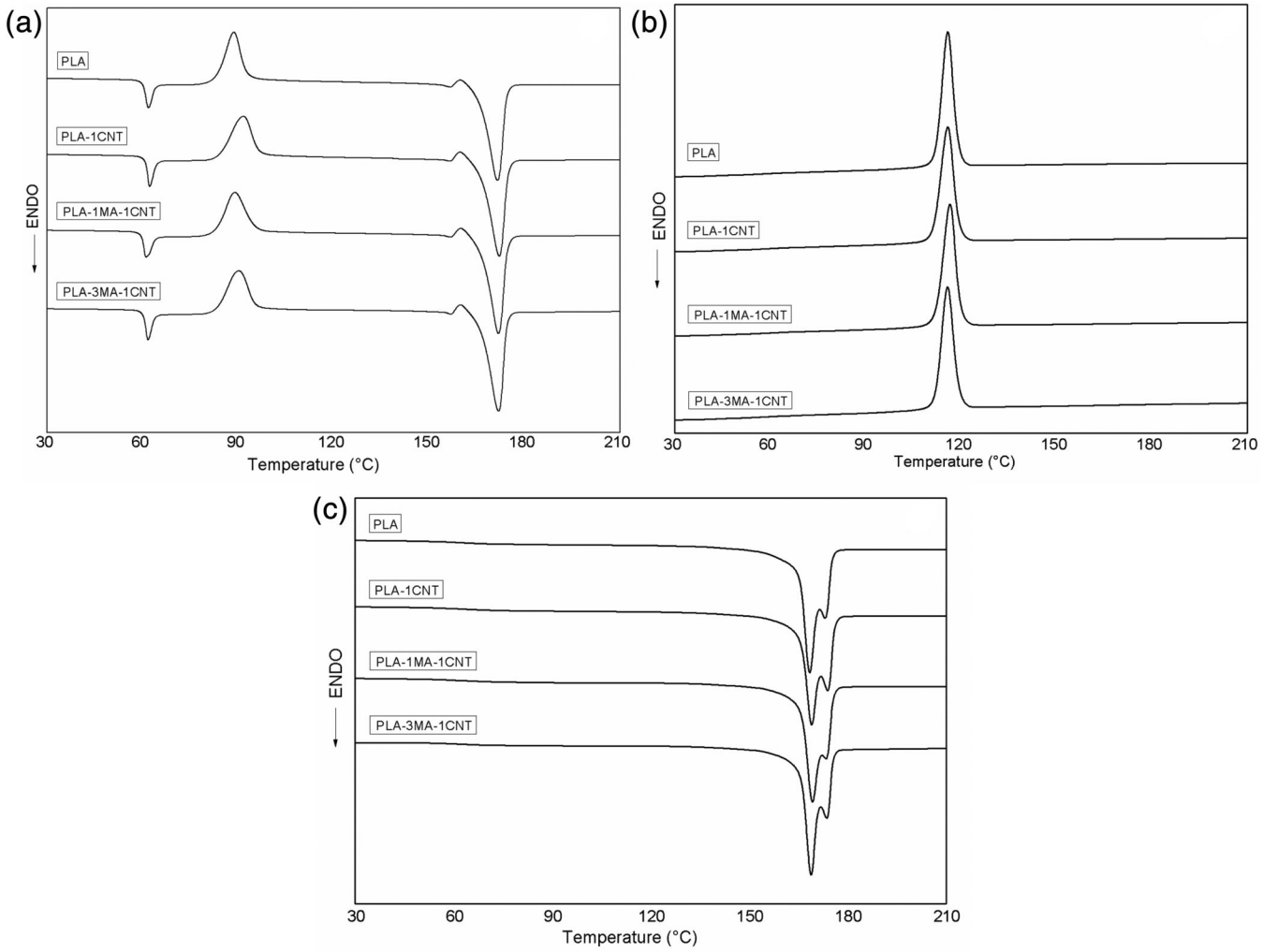

FIGURE 6 DSC curves of PLA and the PLA/CNT nanocomposites with different contents of PLA-*g*-MA: (a) first heating, (b) cooling, and (c) second heating

TABLE 3 Thermal properties obtained by DSC analysis of the PLA and the PLA/CNT nanocomposites with differents contents of PLA-*g*-MA

	First heating				Cooling	Second heating			
Samples	T_g (°C)	T_{cc} (°C)	T_m (°C)	X_{c1} (%)	T_c (°C)	T_g (°C)	T_{m1} (°C)	T_{m2} (°C)	X_{c2} (%)
PLA	61	89	172	23	116	60	168	173	66
PLA-1CNT	62	92	172	24	116	61	169	174	62
PLA-1MA-1CNT	60	89	172	23	117	61	169	173	63
PLA-3MA-1CNT	61	90	172	26	116	61	169	173	63

samples, and it was necessary to use 2.75 J hammer for the other samples. The tests were performed on unnotched samples. A minimum of five samples of each composition was tested.

Tensile tests were carried out according to ASTM D882-12[42] using an MTS test machine (Criterion 42 model), with a load of 250 N, and crosshead speed of 0.1 mm/min. A minimum of seven samples of each composition was tested.

The statistical analysis of mechanical data was carried out using GraphPad Prism version 6.0, through the analysis of variance (ANOVA). Tukey's Honestly Significant Difference (HSD) was used at the 95% confidence level for multiple comparison tests.

2.5.3 | Morphological analysis: Field emission gun scanning electron microscopy

The fracture surfaces of the nanocomposites PLA-1NTC (without compatibilizer agent) and PLA-3MA-1NTC (with compatibilizer agent) were analyzed by FEG-SEM Philips microscopy, model XL30 FEG, operating at 5 kV. The samples were coated with a thin layer of gold to enable the analysis.

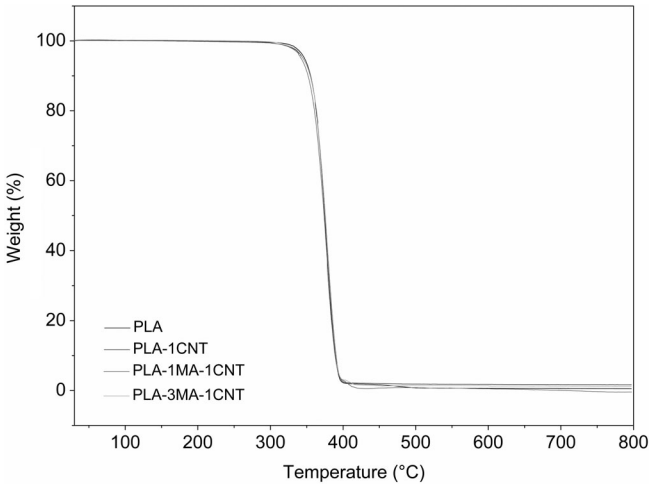

FIGURE 7 | Thermal degradation behavior curves of neat PLA, PLA-1CNT, PLA-1MA-1CNT and PLA-3MA-1CNT

3 | RESULTS AND DISCUSSION

3.1 | Characterization of PLA-g-MA

3.1.1 | Melt-grafting mechanism to produce PLA-g-MA

Figure 1 illustrates the melt-grafting mechanism to produce PLA-*g*-MA using benzoyl peroxide (BPO) as initiator and MA as a monomer. One hypothesis is that the grafting reaction of PLA occurs in three stages.[25] In the first stage, the BPO decomposes into two alkoxys radicals through hemolytic fission, energetically subsidized by the presence of heat. Then, PLA has one of its hydrogens removed by the monovalent radical, giving rise to the formation of the alkyl radical, and it can be seen in reaction 2 (Figure 1). MA reacts with the radical formed from the breakdown of its double bond, being incorporated into the polymer chain and giving rise to the PLA-*g*-MA, which can be seen in reaction 3 (Figure 1). In the reactive processing, all reactions happen simultaneously, starting in the feed zone with the temperature and proceeds with the particle friction and the viscous heating.[8]

3.1.2 | FT-IR spectroscopy

Figure 2 shows the FT-IR spectrum in the regions of 500–4000 cm^{-1} of maleic anhydride (MA), PLA and PLA-

TABLE 4 The initial thermal degradation temperature (T_{onset}), the thermal degradation temperature of 10, 50, and 90% of weight loss, the maximum weight loss rate temperature ($T_{máx}$) and the end thermal degradation temperature (T_{endset})

Sample	T_{onset} (°C)	$T_{10\%}$ (°C)	$T_{50\%}$ (°C)	$T_{90\%}$ (°C)	$T_{máx}$ (°C)	T_{ednset} (°C)
PLA	355	355	375	390	379	390
PLA-1CNT	357	354	375	392	379	391
PLA-1MA-1CNT	357	352	374	389	378	389
PLA-3MA-1CNT	356	355	375	392	379	392

TABLE 5 Young's modulus, tensile strength and Izod impact strength of the PLA and PLA/CNT nanocomposites with different contents of PLA-*g*-MA

Samples	Tensile strength (MPa)	Young's modulus (GPa)	Izod impact strength (J/m)
PLA	11.7 ± 0.8^{b}	1.4 ± 0.1^{a}	65 ± 9^{a}
PLA-1CNT	21.7 ± 3.2^{a}	1.2 ± 0.1^{b}	228 ± 13^{b}
PLA-1CNT-1MA	12.8 ± 0.5^{b}	1.2 ± 0.0^{b}	237 ± 3^{b}
PLA-1CNT-3MA	11.3 ± 3.3^{b}	1.6 ± 0.2^{a}	243 ± 4^{b}

Note: Means values ± *SD*. Mean values with different letters in the same column represent significant differences ($p < 0.05$) among the samples according to ANOVA and Tukey's multiple comparison tests.

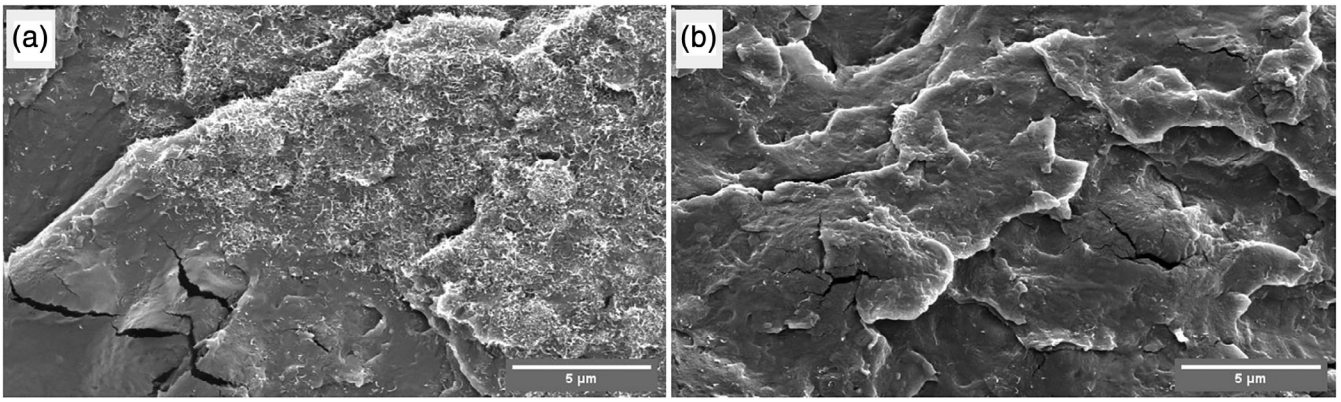

FIGURE 8 FEG-SEM images of PLA/CNT nanocomposites: (a) PLA-1CNT and (b) PLA-3MA-1CNT

g-MA in order to identify the presence of MA on PLA-*g*-MA through comparion of these spectra.

PLA spectra in Figure 2 present CH_3 and CH stretching at 2996 and 2945 cm^{-1}, —C=O carbonyl stretching vibration at 1760 cm^{-1}, CH_3 and CH bending vibrations at 1450, 1379 and 1355 cm^{-1}, asymmetric and symmetric bending vibrations of –C-O-C and –CH_3 rocking at 1186, 1133 and 1043 cm^{-1}, C-C stretching vibration at 950 cm^{-1} and C-COO at 865 cm^{-1}. [44–46] It is possible to observe that the spectra of PLA and PLA-*g*-MA present the same characteristics bands, meaning that the polymer structure was not damaged during the reactive processing with MA.

However, as reported by Orozco et al.,[44] as the concentration of grafted MA is low (2 wt%) the MA characteristic bands, the C=O stretching of maleic acid or anhydride peak, are too weak and might be overlapped with the carbonyl band of PLA.

3.1.3 | Rheological analysis

Figure 3 shows the viscosity as function of the shear rate of PLA, PLA pellet, and PLA-*g*-MA at 180°C. The rheological behavior under low shear rates (0.01–1.0 s^{-1}) is commonly used as an indirect way to understand some structural modifications on polymers. It can be observed for all the samples the Newtonian behavior. The first Newtonian plateau (η_0) is obtained at 0.01 s^{-1}. PLA pellet, PLA and PLA-*g*-MA presented η_0 value around 222, 40 and 8 Pa.s, respectively. The extrusion process decreased η_0 and can be related to the chain break during the processing. The curves of the PLA pellet and PLA do not alter the viscosity with increasing shear rate, indicating a typical Newtonian behavior.[47] The viscosity behavior is related to the molar mass of the material, that is, the lower the molar mass, the lower the viscosity.[8]

Analyzing the behavior of PLA-*g*-MA, it can be seen that there was a significant decrease in η_0 and according to Rigolin et al.,[28] the melt-grafting of MA onto PLA strongly increased acidity content and can promote a reduction in the molar mass of the matrix. The reduction in the viscosity can be also related to the chain break during the processing due the increase of the temperature since the grafting is an exothermic process that contributes to the breakdown of the chains. Besides that, it is also known that PLA-*g*-MA consists of a chain with branches of MA when monomer is grafted into theses activated sites, so these branches aid in resistance to fluid and consequently, they have lower viscosity.[48] The PLA-*g*-MA curve showed a little slight decrease in the viscosity with the increase of the shear rate and presents a trend of pseudoplastic behavior for the analyzed shear rates.

3.1.4 | Thermal analysis: DSC and TGA

Figure 4 shows the thermograms obtained by DSC of the PLA and PLA-*g*-MA during the second heating. Table 1 shows the thermal results: glass transition temperature (T_g) and melting temperature (T_m).

Figure 4 shows the second heating cycle and it is possible observe the presence of T_g and a double T_m peak. Comparing the PLA and PLA-*g*-MA sample, it is possible observe that T_g of PLA-*g*-MA decreased about 20% in relation to PLA. Besides that, the double T_m peaks occur at 169 and 175°C to PLA and at 137 and 152°C to PLA-*g*-MA, so ensure a reduction of 19 and 13% in the T_{m1} and T_{m2}, respectively, with the graphitization of anhydride maleic in matrix PLA. This reduction in temperatures indicates better mobility of chains of PLA-*g*-MA, due to decreased molar mass and increased free volume,[28] generated by the branches of MA grafts in the PLA chain and a possible chain break during processing, justified by the reduction in viscosity as seen in Figure 3.

Figure 5 shows the thermal degradation behaviors for PLA and PLA-*g*-MA and Table 2 shows the initial temperature of thermal degradation (T_{onset}), thermal degradation temperatures of 10, 50 and 90% ($T_{10\%}$, $T_{50\%}$ and $T_{90\%}$) of weight loss, the final temperature of thermal degradation (T_{endset}) and the maximum weight loss rate temperature ($T_{máx}$). The thermal degradation occurred in a single-step process.

In general, PLA and PLA-*g*-MA showed the same behavior, but the PLA-*g*-MA showed a left dislocation of the degradation temperature in relation to the PLA, that is, the sample PLA-*g*-MA have decomposition temperatures which range a few degrees below that of PLA. It is possible that occurred because the maleated samples, normally, are of lower molecular weight.[25] Rigolin et al[28] observed that the chemical modification of PLA with MA decreases molar mass due to chain scission side reaction and the acidity of PLA-*g*-MA is greater because of the grafting of MA in PLA matrix.

3.2 | Effectiveness of PLA-g-MA as an compatibilizer agent for PLA/CNT nanocomposites

Figure 6 shows the thermograms obtained by DSC of the PLA and the nanocomposites during the first heating (Figure 6(a)), cooling (Figure 6(b)), and second heating (Figure 6(c)). Table 3 shows the thermal results: glass transition temperature (T_g), cold crystallization temperature (T_{cc}), melting temperature (T_m), crystallization temperature (T_c), and degree of crystallinity (X_c).

In Figure 6(a) it can be seen that both PLA and PLA/CNT composites with different contents of PLA-*g*-MA have T_g in the range of 61°C. The addition of carbon nanotubes and PLA-*g*-MA did not change the thermal properties of PLA. In addition, PLA and the nanocomposites present an exothermic event that represents a rate of cold crystallization, with heat gain without phase change, during its T_g. PLA has very slow crystallization kinetics and the energy is released with the increase of temperature, reorganization occurs in its structure until the fusion of the polymer.[49–51] No change in the T_{cc} of the PLA with the addition of CNT and PLA-*g*-MA was observed. In general, no thermal parameters were changed. The T_{cc} takes place at a temperature below T_m, thus during the first heating, it is also possible to observe T_m at 172°C in PLA and nanocomposites samples.[50] All samples present very close X_c values (23–26%). A slight increase in X_c was observed with the addition of 3 wt% of PLA-*g*-MA. Figure 6(b) shows the cooling cycle, and it is possible to observe the T_c of PLA and nanocomposites samples at 116–117°C, and no changes were observed with the addition of CNT and PLA-*g*-MA.

Figure 6(c) shows the second heating cycle, it is possible to observe in the presence of T_g and double T_m peak, The T_{cc} peak disappeared in the second cycle once the cooling rate was controlled. The T_g values in the second heating are similar to the first heating. It is also possible to observe a double T_m peak in 168–169°C and 173–174°C, respectively, and can be related with the cold crystallization, since in the second heating the crystalline structures have enough time to reorganize since the heating rate is low and controlled cooling, and so, the double T_m peak can be related to the melting of the least and the most perfect crystals.[51]

In Table 3, it is possible to observe the X_c in second heating around 66 and 62–63% to PLA and nanocomposites, respectively. Comparing with the X_c in first heating, ensure that the PLA sample in second heat increased 186% in relation to the first heat. The X_c of the nanocomposites samples in the second heat also increased by 158%. The controlled cooling rate facilitated the crystallization of the PLA. In this case, the addition of carbon nanotubes slightly decreases the X_c values. It may be an indication that under controlled cooling conditions, the CNT can hinder crystallization. However, the crystallinity values are close to the PLA values. Thus, the addition of the compatibilizer agent did not alter the characteristic temperatures of the PLA.

Figure 7 shows the thermal degradation behaviors for PLA and nanocomposites. Moreover, thermal degradation occurred in a single-step process. Table 4 shows the initial temperature of thermal degradation (T_{onset}), thermal degradation temperatures of 10, 50, and 90% ($T_{10\%}$, $T_{50\%}$, and $T_{90\%}$) of weight loss, the final temperature (T_{endset}) and the maximum weight loss rate temperature (T_{max}).

In general, all compositions showed the same behavior and the degradation temperatures are very close. The addition of 1 and 3 wt% of PLA-*g*-MA and 1 wt% CNT did not modify the thermal decomposition behavior of PLA because all samples had a very similar thermal decomposition at $T_{10\%}$, $T_{50\%}$, and $T_{90\%}$. The addition of PLA-*g*-MA did not alter the thermal stability of PLA.

Table 5 shows the mechanical results, such as tensile strength, Young's modulus and Izod impact strength of PLA and the PLA/CNT nanocomposites with different contents of PLA-*g*-MA. It is possible to observe that the addition of CNT in the PLA matrix caused an increase in the tensile strength, confirming the reinforcing effect of the nanocomposites[52] (increased about 85%, $p < 0.0001$). On the other hand, the addition of PLA-*g*-MA decreases the tensile strength of the nanocomposites, reaching similar values to PLA. The addition of compatibilizer agents

with maleic anhydride has been extensively studied for several systems.[11,53–54] Mechanical reinforcement depends not only on the type and amount of filler but also on the amount of compatibilizer agent added. The maleation effect contributes to a decrease in the mechanical property of the PLA-*g*-MA and, as a consequence, there is a decrease in the mechanical properties of the nanocomposite. Due to the maleation effect,[11,53–54] PLA-*g*-MA is relatively softer than PLA, and this modification can be very interesting when evaluating the impact resistance.

The addition of 1 wt% CNT decreases the elastic modulus when compared to PLA ($p = 0.0182$), and this fact may be related to the great tendency of CNT agglomeration when added in large quantities, as observed by Braga et al.[10] On the other hand, the addition of PLA-*g*-MA contributes to the dispersion/distribution of CNT once the addition of 3 wt% PLA-*g*-MA increases the elastic modulus, which becomes comparable to PLA.

Regarding the results of Izod impact strength tests, it was noted that the addition of CNT in the PLA matrix increased the impact strength when compared to PLA ($p < 0.0001$). PLA is a very fragile polymer, the addition of CNT contributed to the improvement of this property, obtaining an increase of about 250% with the addition of 1 wt% CNT, and an increase of 265% and 274% with the addition 1 and 3 wt % of PLA-*g*-MA, respectively. The better distribution and uniform dispersion of CNT in the PLA matrix, caused by the addition of PLA-*g*-MA, and the maleation effect may have contributed to this significant improvement in mechanical properties.[26]

Figure 8 shows FEG-SEM images of the PLA/CNT nanocomposites with 3 wt% of PLA-*g*-MA and without the addition of compatibilizer agent (PLA-*g*-MA). It was possible to observe that the addition of PLA-g-MA increases the distribution of CNT in the PLA matrix. In Figure 8(a) it is possible to observe the presence of CNT clusters on the surface of the nanocomposite whereas in the Figure 8(b) it is possible to observe good distribution and dispersion of CNT in the PLA matrix with the addition of 3 wt% of PLA-*g*-MA and the presence of large clusters of CNT is not observed, proving the effectiveness of the compatibilizer agent. The good distribution of CNTs in the PLA matrix is responsible for the improvement of the mechanical properties.

4 | CONCLUSIONS

PLA-*g*-MA was successfully prepared by reactive extrusion using benzoyl peroxide as an initiator. The effectiveness of this compatibilizer agent was evaluated for PLA/CNT nanocomposites. The PLA-*g*-MA present lower viscosity compared to PLA, which justifies the temperatures decreased in the T_g and T_m and a small left dislocation of degradation temperature in relation to PLA. For the nanocomposites, the addition of CNT and PLA-*g*-MA does not alter the thermal properties and degradation of the PLA. Besides that, the mechanical properties results showed a significant increase in Izod impact strength due to maleation effect and the better distribution of CNT in the PLA matrix, as shown in the FEG-SEM images. So, the use of the PLA-*g*-MA as a compatibilizer agent for PLA/CNT nanocomposites proved efficient.

ACKNOWLEDGMENTS

The authors are grateful to CNPq (Conselho Nacional de Desenvolvimento Científico e Tecnológico, process 310196/2018-3 and 405675/2018-6) for the financial support. The authors are grateful to Matheus Domingues Silva for help in the elaboration of Figure 1 and Dr. Eduardo Henrique Backes for the FEG-SEM images.

ORCID

Fabio Roberto Passador https://orcid.org/0000-0001-5239-5962

REFERENCES

[1] C. Chang, Y. Cao, J. Yang, G. Zhang, S. Long, X. Wang, J. Yang, *J. Appl. Polym. Sci.* **2019**, *137*, 1.
[2] G. Faludi, G. Dora, K. Renner, J. Móczó, B. Pukánszky, *Compos. Sci. Technol.* **2013**, *89*, 77.
[3] A. E. E. Putra, I. Renreng, H. Arsyad, B. Bakri, *Compos. B* **2020**, *183*, 1.
[4] M. Asgari, M. Masoomi, *Compos. B* **2012**, *43*, 1164.
[5] T. L. Montanheiro, A. do, F. R. Passador, M. P. Oliveira de., N. Duran, A. P. Lemes, *Mater. Res.* **2016**, *19*, 229.
[6] N. G. Gaylord, *J. Macromol. Sci.* **2006**, *26*, 1211.
[7] M. Avella, G. Bogoeva-gaceva, A. Buzarovska, M. E. Errico, G. Gentile, A. Grozdanov, *J. Appl. Polym. Sci.* **2007**, *104*, 3192.
[8] N. F. Braga, H. M. Zaggo, T. L. A. Montanheiro, F. R. Passador, *J. Manuf. Mater. Process.* **2019**, *3*, 37. https://doi.org/10.3390/jmmp3020037.
[9] C. Wu, *J. Appl. Polym. Sci.* **2012**, *123*, 347.
[10] N. F. Braga, H. M. Zaggo, L. S. Montagna, F. R. Passador, *J. Compos. Sci.* **2020**, *4*, 44. https://doi.org/10.3390/jcs4020044.
[11] F. R. Passador, A. C. Ruvolo-Filho, L. A. Pessan, *J. Appl. Polym. Sci.* **2013**, *130*, 1726.
[12] E. Raee, A. Avid, B. Kaffashi, *J. Appl. Polym. Sci.* **2019**, *137*, 1.
[13] N. F. Braga, A. M. LaChance, B. Liu, L. Sun, F. R. Passador, *Adv. Ind. Eng. Polym. Res.* **2019**, *2*, 121.
[14] M.-A. Paoli, in *Degradação e estabilização de polímeros* (Ed: J. C. Andrade) **2008**, Chemkeys, Campinas.
[15] S. M. M. Franchetti, J. C. Marconato, *Quim. Nov.* **2006**, *29*, 811.
[16] X. Pang, X. Zhuang, Z. Tang, X. Chen, *Biotechnol. J.* **2010**, *5*, 1125.
[17] A. J. R. Lasprilla, G. A. R. Martinez, B. H. Lunelli, A. L. Jardini, R. M. Filho, *Biotechnol. Adv.* **2012**, *30*, 321.

[18] P. Bordes, E. Pollet, L. Avérous, *Prog. Polym. Sci.* **2009**, *34*, 125.
[19] T. R. Rigolin, S. H. P. Bettini, *Modificação Química De Poli (Ácido Láctico) Com Anidrido Maleico Por Processamento Reativo*, Universidade Federal de São Carlos, UFSCAR, São Carlos, Brazil **2014**.
[20] S. Lijima, *Nature* **1991**, *354*, 56.
[21] V. Prajapati, P. K. Sharma, A. Banik, *J. Pharm. Sci. Res.* **2011**, *2*, 1099.
[22] A. M. Cassell, J. A. Raymakers, J. Kong, H. Dai, *Am. Chem. Soc.* **1999**, *103*, 6484.
[23] R. Saito, G. Dresselhaus, M. S. Dreselhaus, *Physical Properties of Carbon Nanotubes*, Imperial College Press, London, UK **1998**.
[24] A. C. Fowlks, R. Narayan, *J. Appl. Polym. Sci.* **2010**, *118*, 2810.
[25] D. Carlson, L. Nie, R. Narayan, P. Dubois, *J. Appl. Polym. Sci.* **1999**, *72*, 477.
[26] U. Can, C. Kaynak, *Polym. Compos.* **2020**, *41*, 600.
[27] B.-U. Nam, Y. Son, *J. Appl. Polym. Sci.* **2020**, *137*, e49011.
[28] T. R. Rigolin, M. C. Takahashi, D. L. Kondo, S. H. P. J. Betiini, *Polym. Environ.* **2019**, *27*, 1096.
[29] T. R. Rigolin, L. C. Costa, T. Venâncio, B. Perlatti, S. H. P. Bettini, *Polymer* **2019**, *179*, 1.
[30] A. Akbari, M. Majumder, A. Tehrani, *Handbook of Polymer Nanocomposites. Processing, Performance and Application*, Springer, New York **2015**, p. 282.
[31] D. Wu, L. Wu, M. Zhang, Y. Zhao, *Polym. Degrad. Stab.* **2008**, *93*, 1577.
[32] K. Chrissafis, *Thermochim. Acta* **2010**, *511*, 163.
[33] G.-X. Chen, H.-S. Kim, B. H. Park, J.-S. Yoon, *Macromol. Chem. Phys.* **2007**, *208*, 389.
[34] C.-F. Kuan, H.-C. Kuan, C.-C. M. Ma, C.-H. Chen, *J. Phys. Chem. Solids* **2008**, *69*, 1395.
[35] H.-S. Kim, B. H. Park, J.-S. Yoon, H.-J. Jin, *Eur. Polym. J.* **2007**, *43*, 1729.
[36] J. T. Yoon, S. C. Lee, Y. G. Jeong, *Compos. Sci. Technol.* **2010**, *70*, 776.
[37] C.-S. Wu, H.-T. Liao, *Polymer* **2007**, *48*, 4449.
[38] H.-C. Peng, C.-F. Kuan, C.-H. Chen, K.-C. Lin, H.-C. Kuan, *Adv. Mater. Res.* **2011**, *239–242*, 145.
[39] D. Garlotta, *J. Polym. Environ.* **2001**, *9*, 63.
[40] A. Magiera, J. Markowski, J. Pilch, S. Blazewicz, *J. Nanomater.* **2018**, *2018*, 1.
[41] T. Ceregatti, P. Pecharki, W. M. Pachekoski, D. Becker, C. Dalmolin, *Rev. Matéria* **2017**, *22*, 1.
[42] Standard test method for tensile properties of thin plastics sheeting; **2017**.
[43] Standard test method for determining the izod pendulum impact resistance of plastics; **2015**.
[44] V. H. Orozco, W. Brostow, W. Chonkaew, B. L. López, *Macromol. Symp.* **2009**, *277*, 69.
[45] M. R. A. Moghaddam, S. M. A. Razavi, Y. Jahani, *J. Polym. Environ.* **2018**, *26*, 3202.
[46] T. Yu, N. Jiang, Y. Li, *Compos. A* **2014**, *64*, 139.
[47] A. Masud, J. Kwack, *Comput. Methods Appl. Mech. Eng.* **2011**, *200*, 577.
[48] M. Mihai, M.-T. Ton-That, *Polym. Eng. Sci.* **2014**, *54*, 446.
[49] M. Decol, *Nanocompósitos de poli(ácido lático), poli(ε-caprolactona) e nanotubos de carbono*, Universidade do Estado de Santa Catarina - UDESC, Joinville **2015**.
[50] V. C. Canevarolo Jr., in *Ciência dos Polímeros: um texto básico para tecnólogos e engenheiros*, Artliber, São Paulo, **2013**.
[51] M. Hesami, A. S. Jalali-arani, *Chem. & Ind.* **2017**, *66*, 1564.
[52] S. H. Park, S. G. Lee, S. H. Kim, *Compos. A* **2013**, *46*, 11.
[53] S. Hotta, D. R. Paul, *Polymer* **2004**, *45*, 7639.
[54] M. W. Spencer, L. Cui, Y. Yoo, D. R. Paul, *Polymer* **2010**, *51*, 1056.

How to cite this article: Verginio GEA, Montanheiro TLA, Montagna LS, Marini J, Passador FR. Effectiveness of the preparation of maleic anhydride grafted poly (lactic acid) by reactive processing for poly (lactic acid)/carbon nanotubes nanocomposites. *J Appl Polym Sci*. 2020; e50087. https://doi.org/10.1002/app.50087